Original Research Article

JOURNAL OF RESEARCH

AATCC Journal of Research
2024, Vol. 11(1) 12–19

DOI: 10.1177/24723444231201444
journals.sagepub.com/home/aat
Sage

The Influence of Aging on the Structure and Properties of Composite Materials Based on Polyurethane and Silver Nanoparticles

Eduard A. Lysenkov[1] and Oleksandr V. Striutskyi[2]

Abstract

The aging processes and their influence on structure, thermophysical and antimicrobial properties of polymer nanocomposites based on segmented polyurethane and silver nanoparticles were studied. It was established that an increase in the intensity of intermolecular interactions of polyurethane occurred regardless of the concentration of silver in the silver nanoparticles due to a change in the packing of macromolecules. It was shown that in the process of aging of composites, the effective size of crystallites of polymer matrix decreases and varies in the range of 1.35–1.50 nm. The most pronounced effect of aging is manifested on the melting temperatures of the crystalline phase of polyurethane and the degree of crystallinity. It was found that polyurethane–silver nanoparticle composites exhibit a very high inhibitory capacity against *Staphylococcus aureus*, *Escherichia coli*, and *Candida albicans*. It is shown that aging processes do not affect the antimicrobial characteristics of the studied materials, which indicates their stability. Due to their unique characteristics, synthesized nanocomposite films can be promising for use as antimicrobial coatings in various applications.

Keywords

Aging Effects, Antimicrobial Properties, Polymer Nanocomposites, Polyurethanes, Silver Nanoparticles, Structure, Thermophysical Properties

Introduction

Today, polymer materials have wide practical applications in almost all spheres of human life. A special place is occupied by protective multifunctional coatings based on polymers. Polyurethanes (PUs), which are often used, are one of the most common and promising materials for creating coatings in the textile, leather, and paint industries.[1] PU, an elastomer formed by the reaction of isocyanate and polyether, possesses hard domains dispersed randomly within the soft domains, forming a heterogeneous landscape with a nanosegregated microstructure.[2] In general, the broad range of film hardnesses and high versatility with superior properties such as good adhesion with polymers and low-temperature flexibility have popularized PU as a potential candidate for coatings.[3] In addition, PUs are widely used in the textile industry, in particular for creating textile substrates, waterproof breathable textiles, and protective clothing.[4]

In recent years, due to the risk of the spread of epidemiological diseases, there is a need to develop new antimicrobial coatings based on PUs.[5] Nguyen et al.[6] developed antimicrobial coatings, based on PU. Fe_3O_4–Ag hybrid nanoparticles were homogeneously dispersed into an acrylic PU matrix at a concentration of 0.1%. The antibacterial test showed that the presence of the nanocomposite coating exhibited good antibacterial

[1]Laboratory of Nanocomposite Materials, Petro Mohyla Black Sea National University, Mykolaiv, Ukraine
[2]Institute of Macromolecular Chemistry, National Academy of Sciences of Ukraine, Kyiv, Ukraine

Date Received: 3 May 2023; Revised: 4 August 2023; Accepted: 10 August 2023

Corresponding author:
Eduard A. Lysenkov, Laboratory of Nanocomposite Materials, Petro Mohyla Black Sea National University, 10, 68 Desantnykiv Street, Mykolaiv 54003, Ukraine.
Email: ealysenkov@ukr.net

activity against *Escherichia coli*, whereas no antibacterial activity was observed for the neat coating.

However, one of the main problems of multifunctional PU-based coatings is their instability over time during operation and aging. PU aging may involve physical aging without chemical reactions occurring, chemical changes such as crosslinking during curing of a thermoset, thermal conditioning at elevated temperature, or photochemical aging, as occurs in weathering.[7] Physical aging occurs when a polymer is in a nonequilibrium state and is caused by molecular relaxations that are biased in the direction required to drive the material closer to equilibrium.[8]

Numerical studies were conducted to study the influence of various aging processes[9–11] on PU coatings for automotive interior parts that are frequently exposed to high temperatures, particularly in extreme environments such as deserts and the tropics, which cause thermal aging.[9] Although both physical and chemical processes are involved in aging, it was established that the thermal aging of PU is strongly correlated with the glass transition temperature of the hard segment. Color change and chemical structure degradation of the thermoset PU were observed to increase with aging time.[10] The PU profiles appear to have a rapid color change up to 750 h exposure with a significant decrease in the rate of degradation between 750 and 1000 h. The polymer undergoes a phase separation allowing the soft segment to have more freedom to move. After the breaking of the urethane linkage in the PU chain, the hard segments then undergo enthalpy relaxation. These combined phenomena cause the polymer matrix to retract and expose the surface fibers. To investigate the potential for using nano-reinforced thermoplastic PUs (TPUs) in transparent armor systems to combat premature environmental aging, cellulose nanocrystals (CNCs) sourced from wood pulp were dispersed into PU using planetary ball-milling.[11] The change in thermal response of the PU/CNC nanocomposite is indicative of more restricted PU segments at elevated temperature and therefore improved thermal aging resistance or a change in crystallinity resulting in increased enthalpy of hydrogen bond breaking.

Therefore, the study of aging processes in polymer multifunctional coatings is a very urgent task. Therefore, the purpose of this work was to study the effect of aging on the structure and functional, in particular antimicrobial, properties of PU-based nanocomposite coatings.

Materials and Methods

Materials

The 2-sulfobenzoic acid cyclic anhydride (Merck, $\geqslant 95\%$), 1-methylimidazole (Merck, 99%), $AgNO_3$ (Pharm.), trisodium citrate ($C_6H_5O_7Na_3$, Pharm.), toluene diisocyanate (Merck, mixture of 2,4- and 2,6-isomers in a mass ratio of 4:1), and 1,4-phenylenediamine (Merck, 98%) were used without additional purification; hyperbranched aliphatic oligoester polyol Boltorn®H30 ("Perstorp" Sweden) MM 3500 (equivalent MM of the oligomer by hydroxyl groups, determined by the acylation method, is 117 g/eq.) was purified by reprecipitation from dimethylformamide (DMF) into ether followed by drying in vacuum (1–3 mmHg) at a temperature of 25–30°C for 6 h; polytetramethylene glycol (PTMG) MM 1000 g/mol was kept in a vacuum at a residual pressure of 1-3 mmHg at a temperature of 70–80°C for 6 h; DMF was distilled at a residual pressure of 1–3 mmHg, and ethanol and diethyl ether were used without distillation.

The synthesis of silver nanoparticles (AgNPs) was carried out by the reduction of silver in $AgNO_3$ with trisodium citrate[12] in the presence of (proposed by us) hyperbranched oligomeric ionic liquid (HB-OIL) as their surface stabilizer. HB-OIL was obtained according to our previously developed method[13] by exhaustive acylation of third-generation oligoester polyol (containing 32 terminal aliphatic primary hydroxyl groups) with cyclic 2-sulfobenzoic anhydride and subsequent neutralization of the resulting reaction product with N-methylimidazole. AgNPs were obtained by boiling 0.125 g (0.000734 equivalents (equiv.)) of $AgNO_3$ and 0.731 g (0.002833 equiv.) of $C_6H_5O_7Na_3$ in the presence of 0.941 g (0.002202 equiv.) of HB-OIL in 60 ml of water under reflux for 1 h. The resulting solution was evaporated and the precipitate was evacuated, washed with ethanol, and dried at a residual pressure of 1–3 mmHg at 75–80°C. Product yield was 0.868 g. Fourier transform infrared (FTIR): 660, 735, 762, 802, 841, 879, 906, 1020, 1040, 1053, 1080, 1128, 1138, 1178, 1234, 1265, 1304, 1360, 1393, 1418, 1439, 1475, 1575, 1649, 1718, 2300–3700 (broadened signals of weak intensity) per cm. The synthesized product is a brown powder soluble in water and insoluble in organic solvents. The synthesized product has the abbreviation AgNPs (1:3), which reflects the ratio of silver ions and HB-OIL ionic groups in the initial reaction mixture, respectively.

According to a similar method, NPs were synthesized with a ratio of silver ions and HB-OIL ionic groups in the initial reaction mixture equal to 1:9 with the corresponding abbreviation AgNPs (1:9). At the same time, silver ions were reduced in the composition of 0.044 g (0.000260 equiv.) of $AgNO_3$ using 0.268 g (0.001040 equiv.) of $C_6H_5O_7Na_3$ in the presence of 1.000 g (0.002340 equiv.) of HB-OIL. Product yield was 0.985 g. FTIR: 660, 735, 762, 802, 847, 878, 889, 1020, 1040, 1082, 1138, 1176, 1232, 1258, 1283, 1308,

1337, 1394, 1418, 1441, 1472, 1566, 1574, 1720, 2300–3700 (broadened signals of weak intensity) per cm. The obtained product is a brown powder soluble in water and insoluble in organic solvents.

Preparation of Nanocomposite Polymer Materials PU–AgNPs

The starting PU for obtaining nanocomposites was synthesized in two stages. At the first stage, an isocyanate prepolymer was obtained by the PTMG reaction with a twofold molar excess of toluene diisocyanate by weight at 80°C in a stream of dry nitrogen. The reaction was controlled by the content of isocyanate groups by the titrimetric method. At the second stage, the terminal isocyanate groups of the obtained prepolymer were treated with 1,4-phenylenediamine at a ratio of $NCO:NH_2 = 1:1$ in a 10% solution in DMF until the complete consumption of isocyanate groups according to FTIR spectroscopy. PU was used as a 10% solution in DMF in the preparation of compositions with AgNPs.

Nanocomposite polymer materials PU–AgNPs were obtained by mixing a solution of PU in DMF with an aqueous solution of AgNPs and subsequent evaporation of the mixtures at a temperature of 70–80°C and vacuuming the resulting film materials (residual pressure 3–5 mmHg) at 60–70°C for 4 h. At the same time, the volume ratio of DMF:water was 4:1, respectively, and the content of AgNPs was 2% by mass. The abbreviations PU–AgNPs (1:3)-1 and PU–AgNPs (1:9)-1 are attached to nanocomposite polymer materials obtained using AgNPs (1:3) and AgNPs (1:9). Such materials were examined the next day after they were obtained. The materials that were studied 30 days after they were obtained were designated as PU–AgNPs (1:3)-30 and PU–AgNPs (1:9)-30.

Research Methods

The FTIR spectra were taken on a spectrophotometer "TENSOR 37" (Bruker, Germany) in the spectral range of 600–4000/cm. The structure of the obtained samples was investigated by the method of wide-angle X-ray diffraction on an XRD-7000 diffractometer (Shimadzu, Japan), using CuKa radiation ($\lambda = 1.54$ Å) and a graphite monochromator. The research was carried out by the method of automatic step-by-step scanning in the mode $U = 30$ kB, $I = 30$ mA in the interval of scattering angles from 3.0 to 80 degrees; the exposure time was 5 s. The study of the temperature dependence of the heat flow was carried out in a dry air atmosphere of nitrogen in the temperature range from –100°C to 150°C at a heating rate of 10°C/min by the method of differential scanning calorimetry (DSC) on the DSC-60 Plus device (Shimadzu, Japan). The absolute error in determining the temperature of phase and relaxation transitions was 0.1°C. The antimicrobial activity of AgNPs was studied by the method of diffusion in agar on a solid nutrient medium of Muller-Hinton for bacteria, and Sabouraud's medium for *Candida*. Petri dishes with a nutrient medium were seeded with 10 μL of inoculum of test microorganisms *S. aureus*, *E. coli*, and *C. albicans* at the rate of 10^8 colony-forming units (CFU)/mL. After incubation for 24 h at a temperature of 37°C, the width of the inhibition zone was measured. The antimicrobial activity of nanocomposite coatings was studied by studying the development of colonies of microorganisms on the surface of the material. For this, a test culture of bacteria and fungi with a concentration of microorganisms equal to 10^8 CFU/mL was applied to the coating surface. After 48 h of incubation at a temperature of 37°C, the number of live microorganisms in the inoculum on the surface of the synthesized nanocomposites was studied.

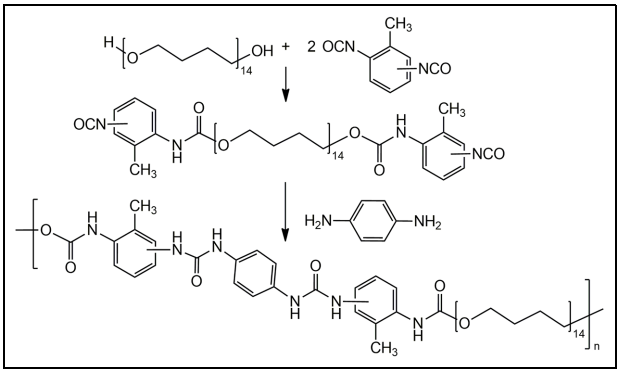

Figure 1. Scheme of PU synthesis.

Results and Discussion

To study the effect of aging on the structure and properties of polymer nanocomposites based on PUs and AgNPs, similar studies of materials were conducted with an interval of 30 days.

PU of a segmented structure (see Figure 1) was used as a matrix polymer for obtaining nanocomposites based on AgNPs in this work. PU was synthesized by a typical scheme, according to which, at the first stage, a prepolymer with terminal isocyanate groups was obtained by PTMG reaction with a twofold molar excess of toluene diisocyanate, and at the second stage, the isocyanate groups of the adduct were blocked with amino groups of 1,4-phenylenediamine. PTMG MM 1000 g/mol was used as a flexible chain component of PU. For the formation of a rigid block, toluene diisocyanate (a mixture of 2,4- and 2,6-isomers in a mass ratio of 4:1, respectively) and 1,4-phenylenediamine

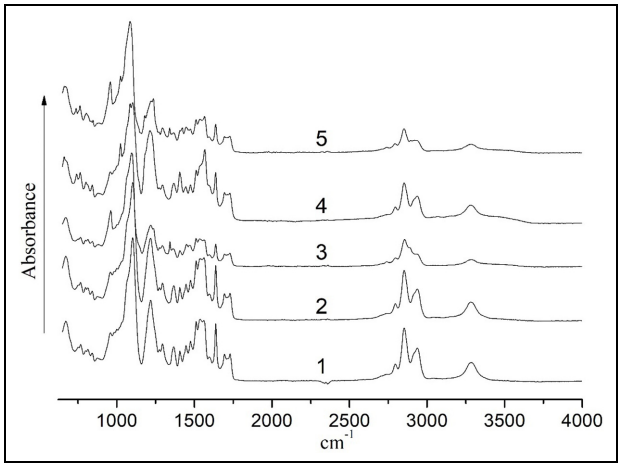

Figure 2. FTIR spectra for unfilled PU (1) and nanocomposites PU–AgNPs (1:3)-1 (2), PU–AgNPs (1:3)-30 (3), PU–AgNPs (1:9)-1 (4) and PU–AgNPs (1:9)-30 (5).

were used. The significant energy of cohesion between rigid blocks formed during their reaction contributes to the formation of the domain microphase structure of PU and ensures their high mechanical characteristics, in particular, the combination of strength and flexibility.

Nanocomposite polymer materials were obtained by combining an aqueous colloidal solution of AgNPs with a solution of PU in DMF followed by removal of solvents. It should be noted that the proposed method of obtaining materials is based on the combination of a matrix polymer and a nanofiller in solution, which contributes to the effective distribution of the latter in the volume of nanocomposites, and is also technological and can be used to form fibers by electrospinning.[14] The content of nanofillers in the composition of the materials was 2% by mass, which according to Lysenkov et al.[15] is sufficient for the manifestation of antimicrobial activity.

It is known that the aging process of polymer, in particular, composite materials, has a significant effect on their structure and properties.[9–11] In this work, the influence of aging of the obtained PU–AgNPs materials for 1 month on their structural features and properties, in particular, antimicrobial activity, was investigated.

The chemical structure of nanocomposite polymer materials, PU–AgNPs, was investigated by the FTIR spectroscopy method. Figure 2 shows the FTIR absorption spectra of the original PU (curve 1) and nanocomposites PU–AgNPs (1:3)-1 (curve 2), PU–AgNPs (1:3)-30 (curve 3), PU–AgNPs (1: 9)-1 (curve 4), and PU–AgNPs (1:9)-30 (curve 5). The spectrum of the initial PU is characterized by absorption bands ν sy C–O–C (958, 999 1099/cm) and ν as C–O–C (1218, 1294/cm) of ether groups, δ sy C–H(CH_3), δ as C–H(CH_3), δ C–H(CH_2) (1407/cm) and ν C–H(CH_2, CH_3), (2723, 2795, 2853, 2936/cm) of methyl and methylene groups, ν ar C–C (1400–1600/cm) of the aromatic component, ν C–N (1367/cm), δN-H, ν sy N–C = O (amide (II) 1512, 1535, 1562/cm), ν NHC = O (amide (I) 1637, 1691, 1730/cm) and ν N–H (3283/cm) of urethane and urea groups.

The spectrum of the PU–AgNPs (1:3)-1 material is almost identical to that of the original PU (curve 1) as a consequence of the weak influence of the interaction of AgNPs with PU on the spectral characteristics of the composite at a given filler concentration. At the same time, there are significant changes in the spectrum of the nanocomposite PU–AgNPs (1:9)-1 (curve 4) compared to the original PU, in particular, the appearance and slight hypsochromic shift of the absorption band ν S = O, C–O–C of the original AgNPs (from 1020 to 1024/cm, see the experimental part, FTIR-spectrum of AgNPs (1:9)), a significant change in the intensities of absorption bands ν ar C–C (1400–1600/cm) of the aromatic component, δN–H, ν sy N–C = O (amide (II) 1512, 1535, 1562/cm), ν NHC = O (amide (I) 1637, 1691, 1730/cm) and ν N–H (3283/cm) of urethane and urea groups, as well as the value of the broadening of the absorption band ν N–H. Such spectral changes indicate the intensive interaction of AgNPs with the rigid block of PU due to the interaction of ionic groups of the stabilizing shell of NPs with urethane and urea groups of PU. After 30 days, the spectra of nanocomposites (PU–AgNPs (1:3)-30 (curve 3) and PU–AgNPs (1:9)-30 (curve 5)) undergo significant changes compared to the original PU and become similar to each other. The specified changes include a significant increase in the intensity of ν as C–O–C at 956/cm, a decrease in the intensity of ν as C–O–C at 1220/cm (for PU–AgNPs (1:9)-30, a hypsochromic shift), ν ar C–C of the aromatic component, δN–H, ν sy N–C = O (amide (II)), ν NHC = O (amide (I)), ν C–H of methyl and methylene groups, as well as a significant decrease in intensity and broadening of the ν N–H absorption band (3283/cm). It should be noted that the absorption band at 1024/cm, which is characteristic of HB-OIL, is preserved for the composite based on AgNPs (1:9). Such spectral changes over time indicate significant changes in the nature of intermolecular interaction in nanocomposites, namely, an increase in the intensity of interaction both between rigid blocks (urethane and urea groups, as well as an aromatic component) and flexible blocks due to a change in the packing of macromolecules, as well as an increase in the intensity of interaction between the modified HB-OIL surface of the AgNPs with flexible and rigid (its urethane and urea groups) PU blocks.

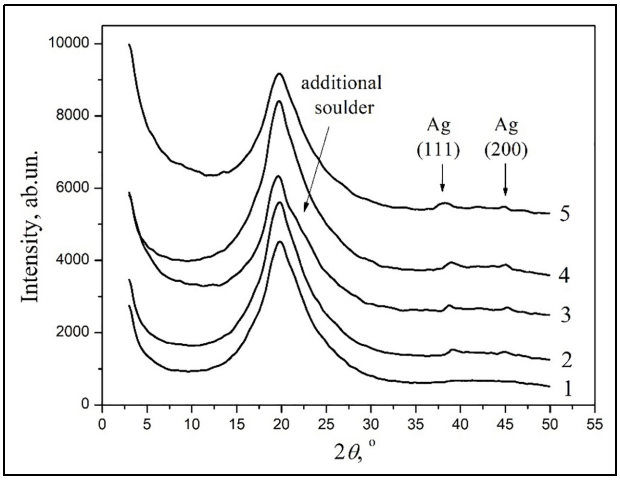

Figure 3. X-ray curves for unfilled PU (1) and nanocomposites PU–AgNPs (1:3)-1 (2), PU–AgNPs (1:3)-30 (3), PU–AgNPs (1:9)-1 (4), and PU–AgNPs (1:9)-30 (5).

The influence of the method of the filler's introduction on the features of structure formation in PU–AgNPs systems at a scale of up to 5 nm was studied by the method of wide-angle X-ray scattering. Figure 2 shows the diffraction curves for unfilled PU and PU-based nanocomposites containing different types of AgNPs introduced by different methods. For unfilled PU, a very wide diffraction maximum is observed in the region of angles from 13° to 30° (Figure 2, curve 1). It is known that PTMG, which is part of PU, is a crystalline polymer, but its crystallinity significantly decreases during polymerization.[16] The reason for the significant decrease in the crystallinity of PTMG is its low molecular weight and the segmented structure of PU (the presence of flexible ether and hard urethane urea blocks). In particular, during the synthesis of PU, PTMG forms flexible oligoether blocks, and toluene diisocyanate in combination with 1,4-phenylenediamine forms hard urethane urea blocks prone to the formation of strong intermolecular bonds with the realization of a microphase-separated structure. The latter causes a significant decrease in the mobility of oligoether segments and, accordingly, their ability to form crystalline structures.[17]

When AgNPs are introduced into the composition of the system, their diffraction curves change (see Figure 2, curves 2–5). A characteristic difference of the diffraction curves for nanofilled on unfilled PU is the presence of two diffraction peaks at 38° and 45°. These maxima indicate the presence of silver crystal structure in the system and correspond to the (111) and (200) planes, respectively.[18] The presence of such maxima in the diffractograms for polymer nanocomposites indicates the presence of AgNPs in their composition. The low intensity of the diffraction peaks of silver is explained by the low contrast between the scattering of the matrix and the filler due to the low content of nanoparticles in the system.

Since PTMG, which is a part of PU, and synthesized AgNPs have a crystalline structure, the effective crystallite size (L) can be calculated for them,[19] using equation (1):

$$L = \frac{k\lambda}{\beta \cos \theta_m} \quad (1)$$

where λ is the wavelength of X-ray radiation; β is the angular spread of the diffraction maximum (in radians), which is usually defined as full width at half maximum (FWHM) after preliminary subtraction of background scattering; k is a coefficient that depends on the crystallite (if the shape is not known, then $k = 0.9$); θ_m is the angular position of the diffraction maximum. FWHM of the most intense maximum at 38° was used to calculate the effective size of crystallites for AgNPs introduced into the polymer matrix

Table 1 shows the values of FWHM, the positions of the maxima, and the crystallite sizes calculated by equation (1) for PTMG and introduced AgNPs.

Table 1 shows that during the formation of the PU matrix, PTMG macromolecules form crystalline structures with an effective size of 1.44 nm. When different types of AgNPs are introduced into PU, the effective size of PTMG crystallites changes. When introducing AgNPs by the dispersion method, the size of crystallites increases compared to unfilled PU to 1.54 nm in the case of AgNPs (1:3) and up to 1.55 nm when filled with AgNPs (1:9). This effect is associated with partial aggregation of nanoparticles, resulting in the formation of larger particles. This leads to a redistribution of interaction energy between molecules and the surface of nanoparticles, while the macromolecules of the flexible PU block become more mobile and can form a larger crystallite. In the process of aging of composites, the effective size of crystallites decreases and varies in the range of 1.35–1.5 nm. Such an effect is evidence that relaxation processes occur in the polymer matrix during the aging process. This leads to the partial release of PTMG macromolecules, which are able to form a crystalline phase. However, in the case of the PU–AgNPs (1:9) system, the crystalline phase increases due to the partial destruction of larger crystals and the formation of smaller crystals. As a result, the effective crystallite size decreases to 1.35 nm. It is also worth noting that an additional shoulder is observed in the 22° region on the diffraction curve for the PU–AgNPs (1:3)-30 system, which may indicate the formation of a new crystalline phase with crystallites of a different type.

By comparing the intensity and FWHM for the diffraction peaks, which are responsible for the structure

Table 1. Values of diffraction peak parameters and calculated crystallite parameters for PTMG and Ag.

Назва	PTMG crystals			Ag crystals		
	θ_m, °	β, °	L, nm	θ_m, °	β, °	L, nm
PU	20.09	5.53	1.44	—	—	—
PU–AgNPs (1:3)-1	20.03	5.18	1.54	38.77	0.85	9.77
PU–AgNPs (1:3)-30	19.95	5.30	1.50	38.75	0.86	9.66
PU–AgNPs (1:9)-1	20.03	5.15	1.55	38.79	0.82	10.13
PU–AgNPs (1:9)-30	19.91	5.91	1.35	38.80	0.83	10.02

PTMG: polytetramethylene glycol; PU: polyurethane; AgNPs: silver nanoparticles.

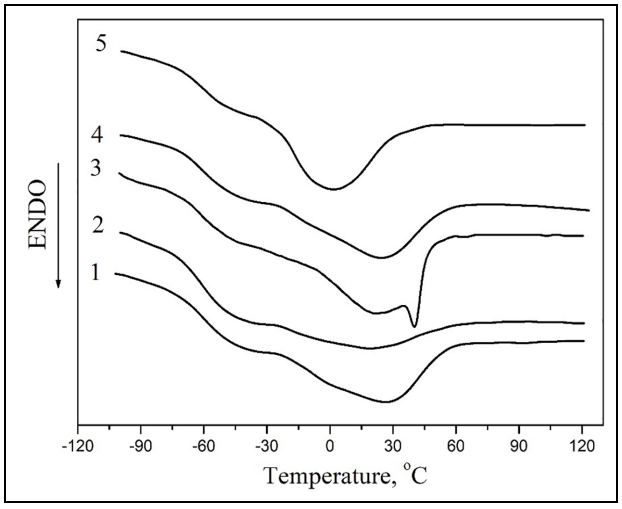

Figure 4. DSC curves for unfilled PU (1) and nanocomposites PU–AgNPs (1:3)-1 (2), PU–AgNPs (1:3)-30 (3), PU–AgNPs (1:9)-1 (4), and PU–AgNPs (1:9)-30 (5).

of silver for systems containing AgNPs (1:3) and AgNPs (1:9), we can conclude that larger silver crystals are formed in AgNPs (1:9). However, it is worth noting that the aging process does not affect the effective size of silver crystallites, because the AgNPs are formed before being introduced into the polymer matrix and do not change their size over time.

Aging processes significantly affect the properties, in particular thermophysical properties, of the obtained PU-based materials. Figure 4 shows the results of DSC for PU-based materials in the temperature range from –100°C to 150°C.

Figure 4 shows that two temperature transitions are observed on the curves for all studied systems: the glass transition, which occurs in the temperature range of –80°C to –30°C and the melting process, in the interval from –30°C to 60°C. The main thermophysical characteristics for the studied materials are given in Table 2.

Figure 3 and Table 2 shows that the introduction of AgNPs with different stabilizer content significantly affects the final thermophysical properties of the obtained nanocomposites. The introduction of AgNPs leads to a decrease in the glass transition temperature of the PU matrix, which is a typical effect of plasticization. At the same time, AgNPs reduce the cooperative mobility of PU macromolecules. A boundary layer of PU molecules is formed around the nanoparticles, which are sterically restricted and lose their mobility. This leads to a decrease in the share of PU polymer chains that are capable of glass transition, which is indicated by a decrease in the heat capacity jump during glass transition (ΔC_p; see Table 2).

Table 2 also shows that aging processes significantly affect the thermophysical characteristics of composites. As a result of aging, the glass transition temperature changes, which decreases by 1.5°C for systems filled with AgNPs (1:9). This effect is associated with the relaxation of PU macromolecules, which makes them more mobile. However, the most pronounced effect of aging is manifested on the melting temperatures of the crystalline phase of PU and the degree of crystallinity. Figure 4 (curve 3) shows that over time an additional crystalline phase is formed in the PU–AgNPs (1:3) system, which is indicated by the presence of two crystalline maxima on the DSC curve. This additional phase is formed in the polymer-filler transition layer and has a melting point of 40.3°C. However, the reverse effect is observed in the aging process for the PU–AgNPs (1:9) system: the melting temperature decreases from 26.3°C to 1.8°C (Figure 4, curve 5). This is due to the formation of smaller crystallites, the melting of which requires less energy.

The degree of crystallinity of nanocomposites based on PU and AgNPs was calculated from the dependence of heat flow on temperature using the equation:

$$\chi_c = \frac{\Delta H_m}{\Delta H_{m,c}} \quad (2)$$

Table 2. Thermophysical characteristics of PU-based nanocomposite materials.

	T_g, °C	ΔC_p, J/(g·°C)	T_m, °C	ΔH_m, J/g	χ, %
PU	−57.9	0.12	28.4	7.4	8.4
PU–AgNPs (1:3)-1	−60.2	0.10	24.1	4.1	4.6
PU–AgNPs (1:3)-30	−60.0	0.11	24.5/40.3	24.2	27.5
PU–AgNPs (1:9)-1	−59.7	0.10	26.3	5.4	6.1
PU–AgNPs (1:9)-30	−61.1	0.10	1.8	18.3	20.8

PU: polyurethane; AgNPs: silver nanoparticles.

where ΔH_m is the measured melting enthalpy and $\Delta H_{m,c}$ is the melting enthalpy of 100% crystalline polymer (for PTMG, $\Delta H_{m,c} = 88$ J/g).[20]

Over time, the degree of crystallinity increases in PU–AgNPs systems (see Table 2). Thus, in the case of PU–AgNPs (1:3), χ increases from 4.6% to 27.5%, and in the case of PU–AgNPs (1:9), χ increases from 6.1% to 20.8%. This effect is explained by relaxation processes that partially release the macromolecules of the flexible PU block, which, in turn, are able to form a crystalline phase. It is also worth noting that with further aging (more than 30 days), the structure and thermophysical properties of the PU–AgNPs systems almost did not change.

As known, AgNPs have high antimicrobial activity. Therefore, the next stage of our work was the study of the inhibitory ability of polymer nanocomposite coatings that contained AgNPs.

Before studying the antimicrobial properties of PU materials, the influence of nanoparticles in powder form on gram-positive, gram-negative bacteria and mycotic flora was studied by the disk diffusion method. It was established that AgNPs show a very high inhibitory capacity against *S. aureus*, *E. coli*, and *C. albicans*. At the same time, for AgNPs, the width of the inhibition zone for *S. aureus* was 30 mm, for *E. coli* it was 12 mm, and for *C. albicans* it was 34 mm.

To study the antimicrobial properties of the obtained nanocomposite PU materials, the ability of test cultures of microorganisms to form a biofilm at the boundary of the solid–gas phase was investigated. For this, a test culture of bacteria and fungi with a concentration of microorganisms equal to 10^8 CFU/mL was applied to the coating surface. After 48 h of incubation, the number of live microorganisms in the inoculum on the surface of the synthesized nanocomposites was studied. The results of the research are given in Table 3.

The obtained results (see Table 3) show that the synthesized nanocomposite materials exhibit antimicrobial properties. Table 3 shows that the aging processes do not affect the antimicrobial characteristics of the studied materials, which indicates their stability. This fact makes the developed materials promising antimicrobial materials suitable for long-term use.

Table 3. Concentration of microorganisms in the inoculum on the surface of the studied materials 48 h after incubation.

	S. aureus (CFU/mL)	*E. coli* (CFU/mL)	*C. albicans* (CFU/mL)
PU	5×10^7	8×10^7	1×10^7
PU–AgNPs (1:3)-1	4×10^5	7×10^5	4×10^4
PU–AgNPs (1:3)-30	3×10^5	7×10^5	4×10^4
PU–AgNPs (1:9)-1	7×10^5	2×10^6	4×10^4
PU–AgNPs (1:9)-30	7×10^5	3×10^5	4×10^4

PU: polyurethane; AgNPs: silver nanoparticles.

Conclusion

The effect of aging processes on the structure and properties of nanocomposite systems based on PUs and AgNPs was studied. FTIR-spectroscopy data indicate an increase in the intensity of interaction of AgNPs with urethane and urea groups of the PU hard block with a decrease in silver concentration in AgNPs. Changes in the FTIR spectra of nanocomposites during their aging indicate an increase in the intensity of intermolecular interactions of PU regardless of the concentration of silver in the AgNPs due to a change in the packing of macromolecules, which is accompanied by an increase in the intensity of interaction between the modified HB-OIL surface of the AgNPs with both flexible and rigid (its urethane and urea groups) PU blocks.

It was established that in the process of aging of composites, the effective size of crystallites decreases and varies in the range of 1.35–1.50 nm. Such an effect is evidence that relaxation processes occur in the polymer matrix during the aging process. This leads to the partial release of PTMG macromolecules, which are able to form a crystalline phase. However, in the case of the PU–AgNPs (1:9) system, the crystalline phase increases due to the partial destruction of larger

crystals and the formation of smaller crystals. As a result, the effective crystallite size decreases to 1.35 nm.

It is shown that the most pronounced effect of aging is manifested on the melting temperatures of the crystalline phase of PU and the degree of crystallinity. It has been established that over time an additional crystalline phase is formed in the PU–AgNPs (1:3) system. This additional phase is formed in the polymer-filler transition layer. However, the opposite effect is observed in the aging process for the PU–AgNPs (1:9) system: the melting temperature decreases by 24°C. This is due to the formation of smaller crystallites, the melting of which requires less energy. It was found that PU–AgNPs composites exhibit a very high inhibitory capacity against *S. aureus*, *E. coli*, and *C. albicans*. The concentration of all types of microbes is significantly reduced when the PU systems are filled. Compared to the initial concentration of microorganisms equal to 10^8 CFU/mL, their concentration decreased by two decimal orders in the case of bacteria and by three orders in the case of mycotic flora. It is shown that aging processes do not affect the antimicrobial characteristics of the studied materials, which indicates their stability.

Declaration of conflicting interests

The author(s) declared no potential conflicts of interest with respect to the research, authorship, and/or publication of this article.

Funding

The author(s) disclosed receipt of the following financial support for the research, authorship, and/or publication of this article: This work was supported by the Ministry of Education and Science of Ukraine from the state budget [State registration number 0122U002326,2022-2023].

References

1. Chow WS, Gan I and Khoo SH. Polyurethane dispersion for sustainable coating applications. In: Hashmi MSJ (ed.). *Encyclopedia of materials: plastics and polymers*. Amsterdam, The Netherlands: Elsevier, 2022, pp. 411–424
2. Iqbal N, Tripathi M, Parthasarathy S, et al. Polyurea coatings for enhanced blast-mitigation: a review. *RSC Adv* 2016; 6: 109706–109717.
3. Rane A, Ajitha AR, Aswathi MK, et al. Applications of waste poly (ethylene terephthalate) bottles. In: Thomas S, Rane AK, Kanny AVK and Thomas MG (eds.). *Recycling of polyethylene terephthalate bottles*. Cambridge: William Andrew Publishing, 2019, pp. 169–189
4. Sikdar P, Dip TM, Dhar AK, et al. Polyurethane (PU) based multifunctional materials: emerging paradigm for functional textiles, smart, and biomedical applications. *J Appl Polym Sci* 2022; 139: e52832.
5. Wang C, Mu C, Lin W, et al. Functional-modified polyurethanes for rendering surfaces antimicrobial: an overview. *Adv in Col Interface Sci* 2020; 283: 102235.
6. Nguyen TNL, Do TV, Nguyen TV, et al. Antimicrobial activity of acrylic polyurethane/Fe3O4-Ag nanocomposite coating. *Prog Org Coat* 2019; 132: 15–20.
7. White JR. Polymer ageing: physics, chemistry or engineering? Time to reflect. *C R Chim* 2006; 9: 1396–1408.
8. Vala AU, Rane AV, Kanny K, et al. Ageing behavior of polyurethane based blends and interpenetrating polymer networks. In: Thomas S, Datta J, Haponiuk JT and Reghunadhan A (eds.). *Polyurethane Polymers*. Amsterdam, The Netherlands: Elsevier, 2017, pp. 261–281.
9. Jeong JH, Seo J, Kim M, et al. Rheology and FTIR-based tools for analyzing thermal-induced physical aging of polyurethane coatings for automotive interior plastic parts. *Prog Org Coat* 2023; 177: 107412.
10. Nicholas J, Mohamed M, Dhaliwal GS, et al. Effects of accelerated environmental aging on glass fiber reinforced thermoset polyurethane composites. *Compos Part B: Engin* 2016; 94: 370–378.
11. Loh TW, Tran P, Das R, et al. Thermoplastic polyurethane-cellulose nanocomposite for transparent armour: characterisation of adhesion and thermal aging. *Compos Commun* 2020; 22: 100465.
12. Rivas L, Sanchez-Cortes S, García-Ramos JV, et al. Growth of silver colloidal particles obtained by citrate reduction to increase the Raman enhancement factor. *Langmuir* 2001; 17(3): 574–577.
13. Shevchenko VV, Stryutsky AV, Klymenko NS, et al. Protic and aprotic anionic oligomeric ionic liquids. *Polymer* 2014; 55(16): 3349–3359.
14. Zhao DM, Feng QM, Lv LL, et al. Fabrication and characterization of cellulose acetate ultrafine fiber containing silver nanoparticles by electrospinning. *Adv Mat Res* 2011; 337: 116–119.
15. Lysenkov E, Stryutsky O and Polovenko L. Development of nanocomposite antimicrobial polymeric materials containing silver nanoparticles. In: *12th international conference "nanomaterials: applications and properties,"* Krakow, Poland, 11–16 September 2022, pp. 1–4. New York: IEEE.
16. Luo K, Wang L, Chen X, et al. Biomimetic polyurethane 3D scaffolds based on polytetrahydrofuran glycol and polyethylene glycol for soft tissue engineering. *Polymers* 2020; 12: 2631.
17. Qin Z, Yunhui L and Kevin CC. Surface biocompatible modification of polyurethane by entrapment of a macromolecular modifier. *Colloids Surf B Biointerfaces* 2013; 102: 345–360.
18. Meng Y. A sustainable approach to fabricating Ag nanoparticles/PVA hybrid nanofiber and its catalytic activity. *Nanomaterials* 2015; 5: 1124–1135.
19. Seo D, Yoo C, Chung IS, et al. Shape adjustment between multiply twinned and single-crystalline polyhedral gold nanocrystals: decahedra, icosahedra, and truncated tetrahedra. *J Phys Chem C* 2008; 112(7): 2469.
20. Xie H, Wu L, Li BG, et al. Poly (ethylene 2,5-furandicarboxylate-mb-poly (tetramethylene glycol)) multiblock copolymers: from high tough thermoplastics to elastomers. *Polymer* 2018; 155: 89–98.